Conformational triggering in voltammetry and single-molecule conductivity of two-centre redox metalloproteins: Cytochrome c4 and copper nitrite reductase

Bohr, Henrik; Shim, Irene; Ulstrup, Jens; Xiao, Xinxin

Published in:
Current Opinion in Electrochemistry

DOI (link to publication from Publisher):
10.1016/j.coelec.2022.101137

Publication date:
2022

Document Version
Publisher's PDF, also known as Version of record

Available online at www.sciencedirect.com

ScienceDirect

Current Opinion in Electrochemistry

Review Article

Conformational triggering in voltammetry and single-molecule conductivity of two-centre redox metalloproteins: Cytochrome c_4 and copper nitrite reductase

Henrik Bohr[1], Irene Shim[2], Jens Ulstrup[2] and Xinxin Xiao[2,3]

Abstract

Blue copper enzymes often show no voltammetry themselves, whereas substrate binding triggers strong electrocatalytic signals. Similarly, electrochemical STM only gives strong contrasts when substrate (O_2, NO_2^-) is present. AFM shows that CuNIR on Au(111)-electrodes modified by self-assembled cysteamine monolayers (SAMs) maintains constant height throughout the electrocatalytic range, while NO_2^- triggers substantial enzyme 'swelling'. 'Swelling' does not accord with the crystalline state, which, however, is not the relevant catalytic environment.

With a view on understanding these patterns, we present *ab initio* quantum chemical studies of CuNIR/OH_2 and CuNIR/NO_2^- 740-atom fragments including the type I and type II Cu-centres. Replacing water at the type II centre by nitrite triggers 2-Å Cu–Cu distance increase, according with enzyme 'swelling'. 2 Å Cu–Cu increase would close intramolecular ET entirely, but is compensated by efficient superexchange alignment of closely interacting LUMOs and HOMOs. In the water-bound enzyme these orbitals are separated by unfavourable through-space tunneling regions.

Addresses

[1] Department of Chemical Engineering, Technical University of Denmark, Building 229, Kemitorvet, DK-2800 Kgs. Lyngby, Denmark
[2] Department of Chemistry, Technical University of Denmark, Building 207, Kemitorvet, DK-2800 Kgs. Lyngby, Denmark
[3] Department of Chemistry and Bioscience, Aalborg University, 9220, Aalborg, Denmark

Corresponding author: Ulstrup, Jens (ju@kemi.dtu.dk)

Current Opinion in Electrochemistry 2022, **36**:101137

This review comes from a themed issue on **Fundamental & Theoretical Electrochemistry (2022)**

Edited by **Rama Kant** and **M.V. Sangaranarayanan**

For complete overview about the section, refer Fundamental & Theoretical Electrochemistry (2022)

Available online 13 September 2022

https://doi.org/10.1016/j.coelec.2022.101137

Keywords

Two-centre redox metalloproteins, Voltammetry, Single-molecule *in situ* STM, Single-molecule *in situ* AFM, DFT and Ab initio calculations, Substrate-triggered single-molecule enzyme swelling.

Introduction

Long-range electron transfer (LRET), by hopping or tunnelling between transition metal or organic redox centres through protein 'matter' is long-time known in photosynthesis, respiration, and multi-centre redox enzyme catalysis [1–4]. The ET processes are often accompanied by coupled proton/electron transfer (PCET) [2,5–7], 'cooperative' effects [7–11], and fluctuating tunnelling barriers [2,7]. LRET in metalloproteins is broadly understood and exploited in biosensors and biofuel cells [12,13], but challenges keep emerging.

A long-standing issue is that redox enzymes – blue copper enzymes in particular – often show no voltammetry, whereas binding of enzyme substrate triggers strong electrocatalytic signals, [14–19]. These are associated with the enzyme, as the substrates themselves, say dioxygen in laccases, or nitrite in CuNIR, Figure 1, exhibit no electrochemistry in these potential ranges, Figure 2. Related effects are that ET between the heme groups of di-heme cytochrome c_4 (*Pseudomonas stutzeri*) is not part of cyt c_4 ET with reaction partners in solution [20], but sub-ms *intramolecular* ET channels open on cyt c_4 immobilisation on Au(111)-electrodes modified by thiol-based SAMs [17,20,21], Figure 2.

New bioelectrochemical techniques include single-crystal, atomically planar electrode surfaces and particularly, scanning tunnelling and atomic force microscopy, directly in aqueous biological media (*in situ* STM and AFM) [16–25]. *In situ* STM/AFM has taken mapping of working metalloproteins to single-molecule resolution, and our theoretically framed single-molecule bioelectrochemistry efforts [16,21,22,26] have expanded to the blue copper enzymes laccase (*Streptomyces coelocolor*)

[17] and CuNIR (*Achromobacter xylosoxidans*) [16,26,27] on thiol-based SAM-modified Au(111)-electrode surfaces.

A first CuNIR and laccase observation is that single-molecule mapping substantiates that neither voltammetry nor *in situ* STM contrasts on SAM-modified Au(111)-electrodes are observed when no substrate (O_2 or NO_2^-) is present. Strong electrocatalysis and high single-molecule electronic conductivity appears, however, in the electrocatalytic potential ranges, when O_2 and NO_2^- are present [16,17,19], Figure 2. A second observation is that pure CuNIR on cysteamine SAM-modified Au(111)-electrodes maintains an *in situ* AFM height of about 4 nm [27] approximately the crystallographic dimension [28–32], in the electrocatalytically active potential range. When NO_2^- is present, the enzyme expands by close to one nm in the potential range, where NO_2^- is reduced electrocatalytically to NO, suggesting that protein conformational changes ('swelling') accompanies NO_2^- binding, Figure 2. Conformational changes must also be what causes NO_2^- triggering of *in situ* STM electronic conductivity. Such structural changes do not accord with crystal structures, which point to insignificant changes on nitrite binding [28–32]. The crystallographic state is, however, not the catalytically relevant state [32], due to the quite different enzyme environments. With a view on understanding conformational changes and ET channel opening on single-molecule nitrite binding, we have initiated computational studies of the CuNIR/OH_2 and CuNIR/NO_2^- core structures. We use the simpler two-centre ET heme protein cyt c_4 on thiol-based SAM Au(111) surfaces as a comparison.

Voltammetry and single-molecule *in situ* STM of cyt c_4 and CuNIR

The electronic conductivity – by tunnelling or 'hopping' [1–4] - through redox metalloproteins is determined by redox potentials, reorganisation free energies, and distance and orientation of the centres. 'Cooperativity' [7,9–11] implies that charge injection, or enzyme substrate binding at a given centre affects the microscopic redox potentials, ET rate constants etc. of all the other centres. Hemoglobin [33] and four-heme cytochrome c_3 [34] are examples. Other cases are ET of (*Alcaligenes xylosoxidans*) CuNIR [35] and cytochrome cd_1 [10]. The number of electronic interactions is mostly prohibitive for mapping, but ***two-centre*** proteins are simple enough that complete mapping is within reach [9,11,20]. Other conformational effects are expected, when proteins are immobilised onto electrochemical surfaces. We illustrate here conformationally triggered intramolecular ET by *P. stutzeri* cyt c_4 [9,18–22] and (*A. xylosoxidans)* CuNIR [16,26,27] (Figures 1 and 2).

Cytochrome c_4

190-residue *P. stutzeri* cyt c_4 is organised in two heme domains, with excess negative and positive electrostatic charge in the N- and C-domain, respectively [37], giving a slightly higher redox potential of the C-terminal heme [9,36]. The dipolar structure enables vertical protein immobilisation on SAM-modified Au(111) electrodes via C–domain binding on negatively charged SAMs [18]. Electrostatic and Monte Carlo computations suggest that PCET between the two heme propionates is involved [21,36,37]. ET is thus a borderline case between weakly coupled diabatic and strongly coupled

Figure 1

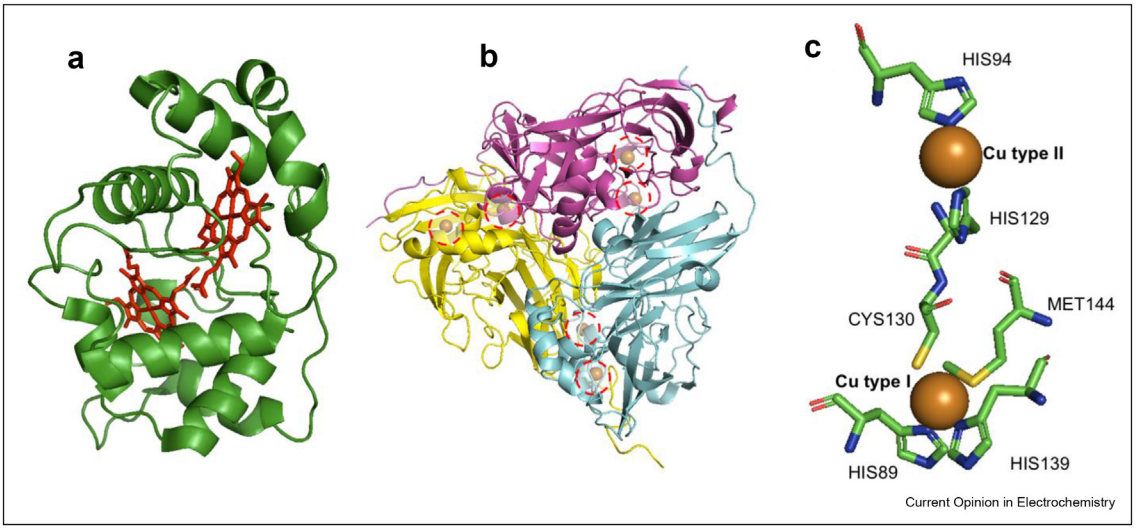

(a) High-resolution structure of *P. stutzeri* cyt c_4 (PB 1ETP). The two heme groups are shown in red. **(b)** High-resolution structure of *A. xylosoxidans* CuNIR trimer (PB 1HAU) viewed along the trigonal axis. The Cu-atoms, encircled by red dashed rings are marked in brown. **(c)** Close-up of the type I and type II Cu-centres in a single monomer.

Figure 2

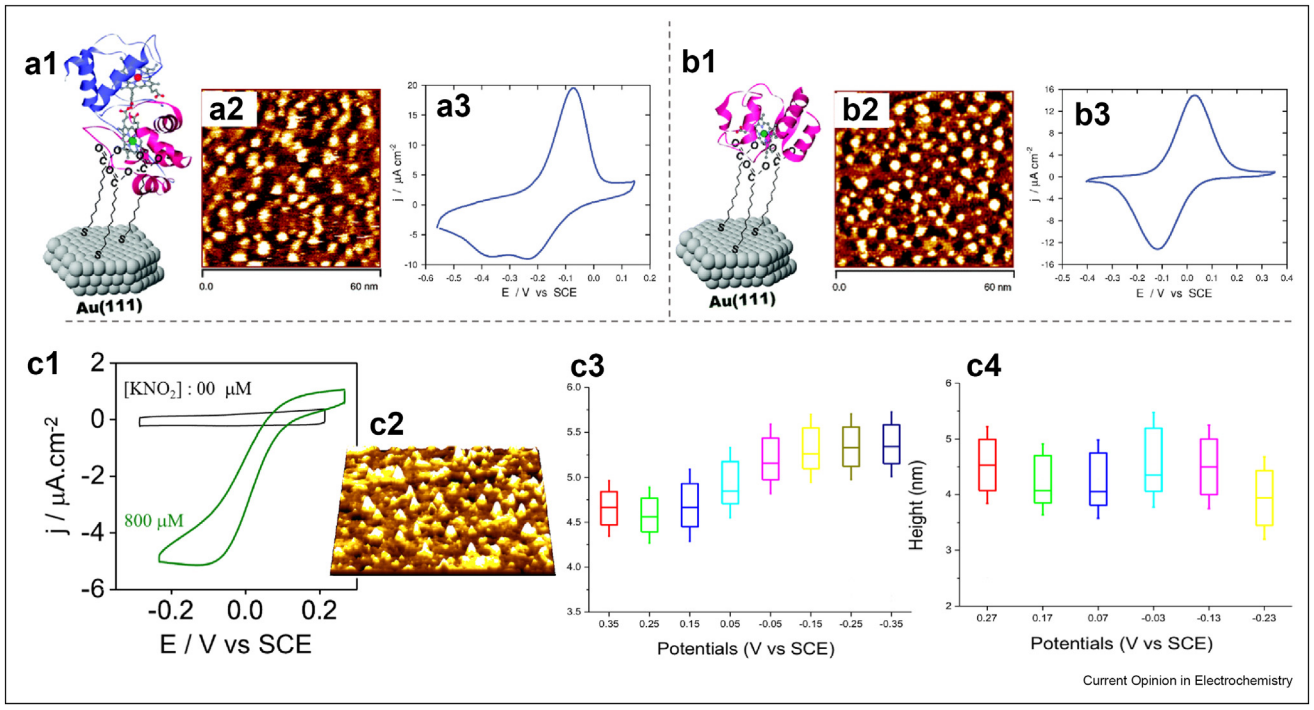

(a) Cyclic voltammetry (CV) and *in situ* STM of *P. stutzeri* cyt c_4. **(b)** CV and *in situ* STM of single-heme horse heart cyt *c* as a comparison. **(c)** CVs (C1) and *in situ* STM (C2) of *A. xylosoxidans* CuNIR. *In situ* electrochemical AFM of *A. xylosoxidans* CuNIR in the presence (C3) and absence (C4) of nitrite.

adiabatic limits, highly sensitive to conformational fluctuations [18,21,38].

ET between cyt c_4 and external reaction partners enabled resolution of all the microscopic thermodynamic and kinetic parameters. Intramolecular ET could not be detected [20], but voltammetry of cyt c_4 vertically oriented via the C-domain on negatively charged Au(111) SAMs, Figure 2 displays intriguing asymmetry, only compatible with (ms to sub-ms) intramolecular ET. Details regarding instrumentation, data, and data analysis are given in Refs. [18,19].

Intramolecular cyt c_4 ET was also addressed by quantum mechanical charge transfer theory [21,38]. The reorganisation free energy is robust to conformational fluctuations, but the electronic transmission coefficient increases by orders of magnitude, when even tiny structural fluctuations take an ET path from the closed crystallographic structure, to thermally accessible non-equilibrium conformations. Highly conspicuous ET 'gating' thus emerges.

The copper enzyme nitrite reductase (*A. xylosoxidans*)

CuNIRs are multimeric two-centre blue Cu-oxidases in the biological N-cycle [28–32]. 'Green' CuNIRs catalyse similar processes [27,39]. In addition to the two-centre nature of the CuNIR subunits, with a type I centre for electron inlet and a catalytic type II centre, there were other rationales for the choice of this single-molecule target protein. The substrate, nitrite is a small molecule, structurally invisible in STM and AFM, but with detectable triggered electronic and conformational enzyme changes. Secondly, both voltammetry in well-defined (single-crystal) environments and high-resolution *in situ* STM and AFM are available for this particular CuNIR target [16,19,22,26,27,40]. CuNIRs catalyse the one-electron reduction at the type II centre [28–32]:

$$NO_2^- + H_2O + e^- \rightarrow NO + 2OH^- \quad (1)$$

This process is essentially a PCET process, and both ET and PT pathways have been explored [16,26,41–44]. Comprehensive crystallographic, spectroscopic, and kinetic studies are reported [28–31,41–44]. Here we focus on intramolecular ET between the type I and type II centres, directly covalently linked via His129-Cys130 ligands, Figure 2. The strong type I–Cys bond ascertains facile superexchange subject to 'gating', either by nitrite binding or enzyme immobilisation. Nitrite 'gated' intramolecular ET and conformational 'swelling', or 'protein quakes' [45] are thus our focus.

Our first frame is high-resolution crystal structures [28–30,36,42–44,46]. Notably, the crystallographic Cu–Cu distances are virtually unchanged on nitrite binding, Table 1. Secondly NO_2^- binding is a prerequisite for electrochemical signals [16,26], although CuNIR alone does give signals on specific SAMs [26]. A third frame is that *in situ* STM of CuNIR on cysteamine-modified Au(111)-surfaces follows CV, i.e. molecular scale *in situ* STM structures ***only*** appear when NO_2^- is present. Finally, single-molecule *in situ* AFM discloses substantial conformational differences ('swelling') when the immobilised enzyme goes from the resting to the active state, Figure 2. This is in contrast to the crystalline state, but as noted this state is not the reactive enzyme state [41].

Solomon and associates analysed intramolecular ET between the type I and type II centres [32,41] in chosen protein fragments using DFT with Hartree–Fock mixing. Focus was on protein dynamics, with subtle gating and dual-path competition. Our focus is also intramolecular ET but with focus on electrochemical nitrite triggering and the pronounced conformational 'swelling' observed by AFM.

A computational approach to *A. xylosoxidans* CuNIR on nitrite binding

We calculated the electronic structure of a 740 atom fragment of the ***A. xylosoxidans*** **CuNIR** type I/type II ET channel and the effects of nitrite binding, using *ab initio* Hartree-Fock self-consistent field methods (HF-SCF). Mobilisation of the full quantum mechanics arsenal is impossible for a protein: the size of CuNIR with more than 9000 atoms not including the H-atoms and 85 Å across the trimer. With the experimental frames noted, we built a model 740 atom *A. xylosoxidans* CuNIR, PDB 1OE1 fragment containing the type I and type II sites. This 33 Å fragment still represents a self-contained protein section. We used HF-SCF in the Roothaan formulation [48] along with the Born-Oppenheimer approximation. Wave functions were Slater determinants, with molecular orbitals (MOs) expanded as linear combinations of atomic orbitals (LCAOs). Gaussian type basis sets were chosen as 6-31G*.

A H_2O molecule was added to the type II Cu(II) centre. As a starting point, the distance between Cu(II) and the O atom of H_2O was set to 2.0 Å. Likewise a NO_2^- ion with a 2.0 Å Cu(II)–N atom distance was added. The fragment structures containing H_2O or NO_2^- were HF-SCF optimised using Gaussian 16 [49]. The calculations converged, when the maximum displacement was less than 0.0018 a.u. and the maximum force was less than 0.00045 a.u. (1 a.u. = 0.53 Å, 82 nN). The converged 740 atom structures were next stripped of the outer amino acids ending with the essential fragments containing the core type I/type II Cu centres with ligands. The final H_2O-bound fragment contained 150 atoms, the NO_2^--bound fragment 148 atoms. Single-point calculations with fixed geometry on these reduced fragments were undertaken. We also calculated *iso*-surfaces of the LUMO (Lowest Unoccupied MO) and five Highest Occupied MOs, HOMO to HOMO–4. The *iso*-values were chosen as 0.02 $(\text{electrons/au}^3)^{1/2}$. Figures 3 and 4 show the resulting electronic and molecular structures of the reduced fragments.

The figures disclose several striking outcomes. One is that the fully optimised NIR structure with nitrite substrate is markedly different from NIR with bound water. Particularly nitrite binding was found to shift the type I and type II centres apart by no less than 2.4 Å, Table 1. This accords with the AFM data, Figure 2, but

Table 1

Overview of some PDB entries of pure and mutant NO_2^- bound CuNIRs. Cu–Cu distances included.

Entry	PDB id	Description	Sequence Length	Cu–Cu distance (Å)	Increase due to nitrite binding (Å)	References
1	2DY2	*Cereibacter sphaeroides* CuNIR at pH 6.0 without nitrite bound	329	12.459	–	[28]
	2DWT	With bound nitrite	329	12.491	+0.032	[28]
2	1WA1	H313Q Mutant of *Achromobacter xylosoxidans* CuNIR nitrite bound	336	12.424	–	[29]
	1WA2	With bound nitrite	336	12.460	+0.036	[29]
3	2PP7	*Alcaligenes faecalis* CuNiR without nitrite bound	341	12.476	–	[30]
	2PP9	With bound nitrite	341	12.574	+0.098	[30]
4	1OE1	*Achromobacter xylosoxidans* CuNIR; Fragment with water optimised	336	12.07	–	[47]
	1OE1	Fragment with NO_2^-optimised	336	14.46	+2.39	[47]

Figure 3

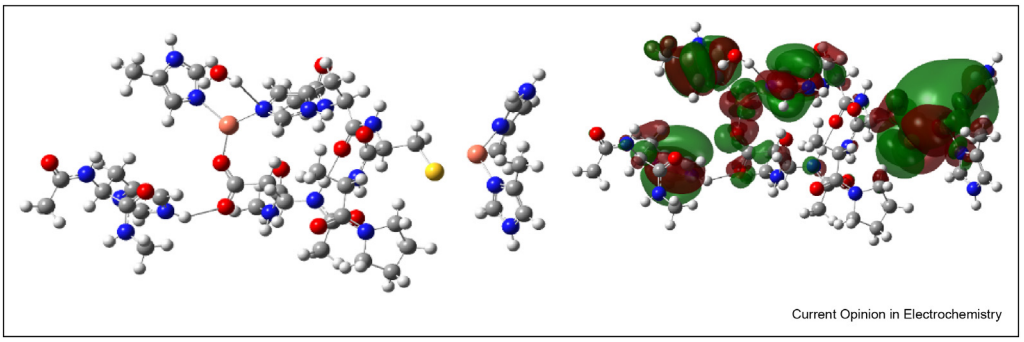

150 atom fragment with bound H_2O. Left: Optimised atomic structure. Right: Fragment with LUMO and HOMO to HOMO–4 isosurfaces (green and red show phases of the orbitals). Ball and stick colours: Grey: carbon; blue: nitrogen; red: oxygen; yellow: sulfur; orange: copper.

at the same might be expected to close the intramolecular ET channel. The structural expansion is, however, compensated by a drastic electronic change in the ET pathway. The conduction orbitals for the water-bound fragment are spatially separated, with conspicuous through-space regions, unfavourable for ET. The NO_2^- fragment orbitals, however, expand to form a channel of nearest neighbour interactions, opening an efficient LRET channel. CuNIR/NO_2^- frontier orbitals are also in an energetically descending line of HOMO states ending with the LUMO state (expanded green−red surfaces), facilitating ET in either direction (electron ***and*** hole transfer).

We calculated the Mulliken charges on all the atoms [50], Table 2. Quantum chemical computations, do not directly provide formal integer atomic oxidation states, as the electrons are delocalised between the metals and the ligands. The Mulliken population analysis of the wave functions shows that both centres for CuNIR/OH_2 have identical oxidation states. Adding NO_2^- to Cu(II) results in charges +0.33 on Cu(I) and +0.67 on Cu(II), Table 2. This can be interpreted as formal oxidation states +1 of Cu(I) and +2 of Cu(II). Charges on individual atoms in chemical compounds are not observables, but the Mulliken analysis is commonly used as measures of charges associated with individual atoms. These charges are, however, unlikely to coincide with the formal charges.

A final − also notable − observation is that neither H_2O nor NO_2^- binds coordinatively to the type II centre, but via 4.3 Å NO_2^- non-covalent bonding via an oxygen atom to an imidazole ring coordinated to the type II Cu-centre. During the optimisation the configuration around Cu(II) is changed considerably. In the final state Cu(II) ends up coordinated to two imidazole rings and a carboxylate group of glutamic acid. Although possibly an artifact of the model used (fragment protein), non-covalent interactions such as

Figure 4

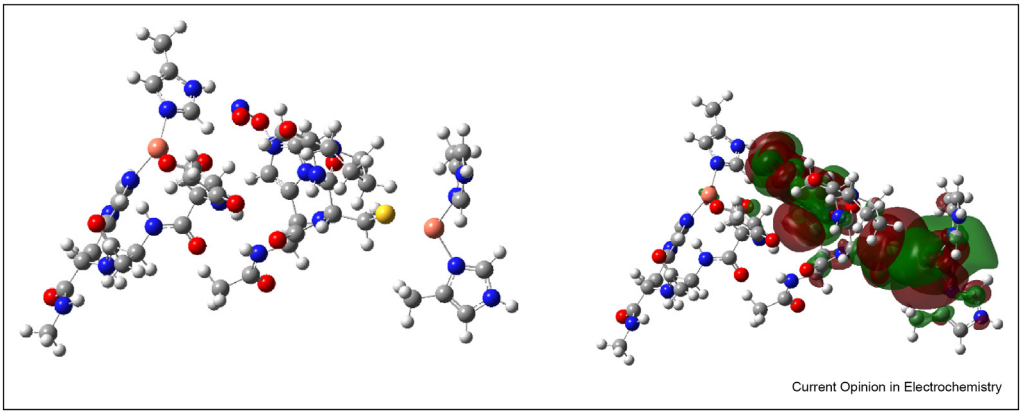

148 atom NO_2^- fragment. Left: Molecular structure. Right: Fragment with LUMO and HOMO to HOMO–4 isosurfaces. Colour code as in Figure 3.

Table 2

Mulliken charges (in units of the electron charge) associated with Cu(I) and Cu(II) for the fragments containing H_2O and NO_2^-, as well as the charges associated with bound H_2O and NO_2^-.

	H_2O	NO_2^-
Cu (I)	0.62	0.33
Cu(II)	0.66	0.67
NO_2^-		−0.83
H_2O	0.01	

these may still be competitive in strength with coordinative bonding [51,52].

Concluding remarks

Immobilisation of composite, multi-centre redox proteins, can lead to drastic changes in the elementary ET kinetic parameters. Such changes are understood in some detail for prototype two-heme cyt c_4 based on fast reaction kinetics, CV at single-crystal SAM modified Au(111)-electrode surfaces, single-molecule *in situ* STM, and DFT. The type I/type II blue CuNIR pattern is less clear-cut. CV at SAM modified Au(111)-electrodes shows nitrite triggered voltammetry, and *in situ* STM exhibits high conductivity ***only*** when nitrite is present. *In situ* AFM shows furthermore significant structural 'swelling', when the enzyme goes from the resting to the active state, where NO_2^- is electrocatalytically reduced to NO. This outcome does not accord with the insignificant crystal structure changes, when NO_2^- is bound.

We have investigated, how large-scale computational efforts can help to resolve this apparent dilemma. Our conclusions are limited by our molecular target necessarily constituting only an enzyme fragment, although strategically designed. Bulk solvent is also absent, although protein-bound water molecules are included. It can be argued that these reservations are no more severe than comparison between densely packed crystalline environments and real CuNIR electrocatalysis in the inhomogeneous, aqueous electrochemical environment.

With these reservations our computations prompt several observations. One is that replacing bound water around the type II centre by nitrite triggers significant increase in the Cu—Cu distance, a couple of Å or so, according with enzyme 'swelling' disclosed by AFM, but > 2-Å Cu—Cu distance increase might be expected to close the intramolecular ET channel. Our computations, however, also show that NO_2^--binding aligns closely interacting LUMOs and HOMOs, compatible with superexchange along nearest-neighbour, closely interacting MOs. In CuNIR/OH_2 these orbitals are separated by unfavourable through-space tunnelling regions. It is, finally notable that the drastic molecular and electronic structural changes appear caused by non-covalent interactions via an imidazole type II ligand, rather than direct coordinative bonding. In the low-dielectric protein environment these two forces can, however, be of comparable strength [51,52].

Cautious overall conclusions are then, first that transfer of the enzyme from the rigid crystalline phase to the solute (or vacuum) state relaxes the structure towards high flexibility and reactivity. Secondly, enzyme 'swelling' accompanies nitrite binding as observed by *in situ* AFM. The increased intramolecular ET distance is compensated by much closer spatial alignment and electronic overlap of the charge transmitting MOs. Finally, the drastic molecular and electronic structural effects appear to be triggered by strong but indirect NO_2^- binding to an imidazole ligand of the type II centre rather than by direct coordination.

Declaration of competing interest

The authors declare that they have no known competing financial interests or personal relationships that could have appeared to influence the work reported in this article.

Data availability

Data will be made available on request.

Acknowledgement

X.X. acknowledges a Villum Experiment (grant No. 35844). Professor Pernille Harris, University of Copenhagen is acknowledged for help with creating the trimer enzyme from the PDB file 1OE1. Professor Günther Peters, DTU Chemistry is acknowledged for introduction to the program Visual Molecular Dynamics (VMD 1.9.1) that enabled us to cut out the 740-atom CuNIR fragment.

References

Papers of particular interest, published within the period of review, have been highlighted as:

* of special interest
** of outstanding interest

1. ** Gray HB, Winkler JR: **Functional and protective hole hopping in metalloenzymes**. *Chem Sci* 2021, **12**:13988–14003.
Detailed and updated review of the physics and mechanisms of electron transport through metalloproteins.

2. ** Nazmutdinov RR, Ulstrup J: **Retrospective and Prospective views of electrochemical electron transfer processes: theory and computations**. In *Atomic-scale modelling of electrochemical systems*. Edited by Melander MM, Laurila TT, Laasonen K, John Wiley & Sons; 2021:27–91.
Updated detailed review with a tutorial touch, of theoretical and computational approaches to interfacial electrochemical macroscopic and single-molecule electron and proton transfer processes.

3. Blumberger J: **Recent advances in the theory and molecular simulation of biological electron transfer reactions**. *Chem Rev* 2015, **115**:11191–11238.

4. * Hammerich O, Ulstrup J: *Bioinorganic electrochemistry*. Dordrecht: Springer; 2007.
Useful overview of a number of electrochemical metalloprotein and DNA-based systems including theoretical approaches to single-molecule bioelectrochemistry.

5. Kuznetsov A, Ulstrup J: **Proton and hydrogen atom tunnelling in hydrolytic and redox enzyme catalysis**. *Can J Chem* 1999, **77**:1085–1096.

6. Warburton RE, Soudackov AV, Hammes-Schiffer S: **Theoretical modeling of electrochemical proton-coupled electron transfer**. *Chem Rev* 2022, **122**:10599–10650.

7. Kuznetsov AM, Ulstrup J: **Theory of Interrelated electron and proton transfer processes**. *Russ J Electrochem* 2003, **39**:9–15.

8. Yan J, Frøkjær EE, Engelbrekt C, Leimkühler S, Ulstrup J, Wollenberger U, Xiao X, Zhang J: **Voltammetry and single-molecule in situ scanning tunnelling microscopy of the redox metalloenzyme Human sulfite oxidase**. *ChemElectroChem* 2021, **8**:164–171.

9. Conrad LS, Karlsson JJ, Ulstrup J: **Electron transfer and spectral α-Band properties of the di-heme protein cytochrome c_4 from *Pseudomonas stutzeri***. *Eur J Biochem* 1995, **231**:133–141.

10. Farver O, Brunori M, Cutruzzolà F, Rinaldo S, Wherland S, Pecht I: **Intramolecular electron transfer in *Pseudomonas aeruginosa* cd_1 nitrite reductase: Thermodynamics and kinetics**. *Biophys J* 2009, **96**:2849–2856.

11. Andersen NH, Harnung SEG, Trabjerg I, Moura I, Moura JJG, Ulstrup J: **Broad-temperature range spectroscopy of the two-centre modular redox metalloprotein *Desulfovibrio desulfuricans* desulfoferrodoxin**. *Dalton Trans* 2003:3328–3338.

12. Tang J, Yan X, Engelbrekt C, Ulstrup J, Magner E, Xiao X, Zhang J: **Development of graphene-based enzymatic biofuel cells: a minireview**. *Bioelectrochemistry* 2020, **134**:107537.

13. Xiao X, Xia H-q, Wu R, Bai L, Yan L, Magner E, Cosnier S, Lojou E, Zhu Z, Liu A: **Tackling the challenges of enzymatic (Bio)Fuel cells**. *Chem Rev* 2019, **119**:9509–9558.

14. * Shleev S, Tkac J, Christenson A, Ruzgas T, Yaropolov AI, Whittaker JW, Gorton L: **Direct electron transfer between copper-containing proteins and electrodes**. *Biosens Bioelectron* 2005, **20**:2517–2554.
Detailed overview up to 2005 of copper protein and enzyme electrochemistry in a variety of local electrode and membrane environments.

15. ** Armstrong FA: **Some fundamental insights into biological redox catalysis from the electrochemical characteristics of enzymes attached directly to electrodes**. *Electrochim Acta* 2021, **390**:138836.
Detailed updated and inspiring overview of physical and chemical aspects of complex redox proteins, including copper proteins in electrochemical environments.

16. Zhang J, Welinder AC, Hansen AG, Christensen HEM, Ulstrup J: **Catalytic monolayer voltammetry and in situ scanning tunneling microscopy of copper nitrite reductase on cysteamine-modified Au(111) electrodes**. *J Phys Chem B* 2003, **107**:12480–12484.

17. Climent V, Zhang J, Friis EP, Østergaard LH, Ulstrup J: **Voltammetry and single-molecule in situ scanning tunneling microscopy of laccases and Bilirubin oxidase in electrocatalytic dioxygen reduction on Au(111) single-crystal electrodes**. *J Phys Chem C* 2012, **116**:1232–1243.

18. Chi Q, Zhang J, Arslan T, Borg L, Pedersen GW, Christensen HEM, Nazmudtinov RR, Ulstrup J: **Approach to interfacial and intramolecular electron transfer of the Diheme protein cytochrome c_4 assembled on Au(111) surfaces**. *J Phys Chem B* 2010, **114**:5617–5624.

19. * Zhang J, Kuznetsov AM, Medvedev IG, Chi Q, Albrecht T, Jensen PS, Ulstrup J: **Single-molecule electron transfer in electrochemical environments**. *Chem Rev* 2008, **108**:2737–2791.
Detailed overview of electrochemical electron transfer and theory of *in situ* scanning tunnelling microscopy imaging and spectroscopy of single molecules and biomolecules.

20. Raffalt AC, Schmidt L, Christensen HEM, Chi Q, Ulstrup J: **Electron transfer patterns of the di-heme protein cytochrome c_4 from *Pseudomonas stutzeri***. *J Inorg Biochem* 2009, **103**:717–722.

21. Nazmutdinov RR, Zinkicheva TT, Shermukhamedov SA, Zhang J, Ulstrup J: **Electrochemistry of single molecules and biomolecules, molecular scale nanostructures, and low-dimensional systems**. *Curr. Opin. Electrochemistry* 2018, **7**:179–187.

22. Engelbrekt C, Nazmutdinov RR, Shermukhamedov S, Ulstrup J, Zinkicheva TT, Xiao X: **Complex single-molecule and molecular scale entities in electrochemical environments: mechanisms and challenges**. *Electrochem. Sci. Adv.* 2021:e2100157.

23. Ha TQ, Planje IJ, White JRG, Aragonès AC, Díez-Pérez I: **Charge transport at the protein–electrode interface in the emerging field of BioMolecular Electronics**. *Curr. Opin. Electrochemistry* 2021, **28**:100734.

24. ** Zhang B, Ryan E, Wang X, Song W, Lindsay S: **Electronic transport in molecular Wires of Precisely Controlled Length built from modular proteins**. *ACS Nano* 2022, **16**:1671–1680.
This report, and the following report (Ref. 25) have opened new approaches to electronic properties of single molecules and biomolecules – including non-redox molecules – in electrochemical environments.

25. Lindsay S: **Ubiquitous electron transport in non-electron transfer proteins**. *Life* 2020, **10**:72.

26. Welinder AC, Zhang J, Hansen AG, Moth-Poulsen K, Kuznetsov AM, Bjørnholm T, Ulstrup J: **Voltammetry and electrocatalysis of *Achromobacter xylosoxidans* copper nitrite reductase on Functionalized Au(111)-electrode surfaces**. *Z Phys Chem (Munich)* 2007, **221**:1343–1378.

27. ** Hao X, Zhang J, Christensen HEM, Wang H, Ulstrup J: **Electrochemical single-molecule AFM of the redox metalloenzyme copper nitrite reductase in action**. *ChemPhysChem* 2012, **13**:2919–2924.
First single-molecule AFM study of a redox metalloprotein in action under full electrochemical control.

28. Adman ET, Murphy MEP: **Copper nitrite reductase**. In *Handbook of metalloproteins*. New York: John Wiley & Sons; 2001:1381–1390.

29. Jacobson F, Pistorius A, Farkas D, De Grip W, Hansson Ö, Sjölin L, Neutze R: **pH Dependence of copper geometry, reduction potential, and nitrite Affinity in nitrite reductase**. *J Biol Chem* 2007, **282**:6347–6355.

30. Barrett ML, Harris RL, Antonyuk S, Hough MA, Ellis MJ, Sawers G, Eady RR, Hasnain SS: **Insights into redox partner interactions and substrate binding in nitrite reductase from Alcaligenes xylosoxidans: crystal structures of the Trp138His and His313Gln mutants**. *Biochemistry* 2004, **43**:16311–16319.

31. Tocheva EI, Eltis LD, Murphy MEP: **Conserved active site residues limit Inhibition of a copper-containing nitrite reductase by small molecules**. *Biochemistry* 2008, **47**:4452–4460.

32. Jones SM, Solomon EI: **Electron transfer and reaction mechanism of laccases**. *Cell Mol Life Sci* 2015, **72**:869–883.

33. Paoli M, Nagai K: **Hemoglobin**. In *Handbook of metalloproteins*. New York: John Wiley & Sons; 2001:16–30.

34. Paquete CM, Turner DL, Louro RO, Xavier AV, Catarino T: **Thermodynamic and kinetic characterisation of individual haems in multicentre cytochromes c_3**. *Biochim Biophys Acta* 2007, **1767**:1169–1179.

35. Leferink NGH, Antonyuk SV, Houwman JA, Scrutton NS, Eady RR, Hasnain SS: **Impact of residues remote from the catalytic centre on enzyme catalysis of copper nitrite reductase**. *Nat Commun* 2014, **5**:4395.

36. Andersen NH, Christensen HEM, Iversen G, Nørgaard A, Scharnagle C, Thuesen MH, Ulstrup J: **Cytochrome c_4**. In *Handbook of metalloproteins*. New York: John Wiley & Sons; 2001:100–109.

37. Kadziola A, Larsen S: **Crystal structure of the dihaem cytochrome c_4 from Pseudomonas stutzeri determined at 2.2 Å resolution**. *Structure* 1997, **5**:203–216.

38. Nazmutdinov RR, Bronshtein MD, Zinkicheva TT, Chi Q, Zhang J, Ulstrup J: **Modeling and computations of the intramolecular**

electron transfer process in the two-heme protein cytochrome c_4. *Phys Chem Chem Phys* 2012, **14**:5953–5965.

39. Nojiri M, Xie Y, Inoue T, Yamamoto T, Matsumura H, Kataoka K, Deligeer N, Yamaguchi K, Kai Y, Suzuki S: **Structure and function of a hexameric copper-containing nitrite reductase**. *Proc Nat Acad Sci* 2007, **104**:4315–4320.

40. Hansen AG, Zhang J, Christensen HEM, Welinder AC, Wackerbarth H, Ulstrup J: **Electron transfer and redox metalloenzyme catalysis at the single-molecule level**. *Isr J Chem* 2004, **44**:89–100.

41. Solomon EI, Hadt RG: **Recent advances in understanding blue copper proteins**. *Coord Chem Rev* 2011, **255**:774–789.

42. Leferink NGH, Han C, Antonyuk SV, Heyes DJ, Rigby SEJ, Hough MA, Eady RR, Scrutton NS, Hasnain SS: **Proton-coupled electron transfer in the catalytic cycle of Alcaligenes xylosoxidans copper-dependent nitrite reductase**. *Biochemistry* 2011, **50**:4121–4131.

43. Hough MA, Eady RR, Hasnain SS: **Identification of the proton channel to the active site type 2 Cu center of nitrite reductase: structural and enzymatic properties of the His254Phe and Asn90Ser mutants**. *Biochemistry* 2008, **47**:13547–13553.

44. Leferink NGH, Pudney CR, Brenner S, Heyes DJ, Eady RR, Samar Hasnain S, Hay S, Rigby SEJ, Scrutton NS: **Gating mechanisms for biological electron transfer: Integrating structure with biophysics reveals the nature of redox control in cytochrome P450 reductase and copper-dependent nitrite reductase**. *FEBS Lett* 2012, **586**:578–584.

45. Ansari A, Berendzen J, Bowne SF, Frauenfelder H, Iben IE, Sauke TB, Shyamsunder E, Young RD: **Protein states and proteinquakes**. *Proc Natl Acad Sci USA* 1985, **82**:5000–5004.

46. ** Hadt RG, Gorelsky SI, Solomon EI: **Anisotropic covalency Contributions to superexchange pathways in type one copper active sites**. *J Am Chem Soc* 2014, **136**:15034–15045.
Detailed DFT analysis of the electronic coupling between the CuNIR type I and type II centres in protein fragments via the protein backbone and hydrogen bond contacts; focus on the protein dynamics on the strong Cu($3dx^2$-y^2)-Sπ(Cys) bond, which is the electron inlet site for the dual-path superexchange ET channels.

47. Ellis MJ, Dodd FE, Sawers G, Eady RR, Hasnain SS: **Atomic resolution structures of native copper nitrite reductase from Alcaligenes xylosoxidans and the active site mutant Asp92Glu**. *J Mol Biol* 2003, **328**:429–438.

48. Roothaan CCJ: **New Developments in molecular orbital theory**. *Rev Mod Phys* 1951, **23**:69–89.

49. Frisch MJ, Trucks GW, Schlegel HB, Scuseria GE, Robb MA, Cheeseman JR, Scalmani G, Barone V, Petersson GA, Nakatsuji H, Li X, Caricato M, Marenich AV, Bloino J, Janesko BG, Gomperts R, Mennucci B, Hratchian HP, Ortiz JV, Izmaylov AF, Sonnenberg JL, Williams, Ding F, Lipparini F, Egidi F, Goings J, Peng B, Petrone A, Henderson T, Ranasinghe D, Zakrzewski VG, Gao J, Rega N, Zheng G, Liang W, Hada M, Ehara M, Toyota K, Fukuda R, Hasegawa J, Ishida M, Nakajima T, Honda Y, Kitao O, Nakai H, Vreven T, Throssell K, Montgomery Jr JA, Peralta JE, Ogliaro F, Bearpark MJ, Heyd JJ, Brothers EN, Kudin KN, Staroverov VN, Keith TA, Kobayashi R, Normand J, Raghavachari K, Rendell AP, Burant JC, Iyengar SS, Tomasi J, Cossi M, Millam JM, Klene M, Adamo C, Cammi R, Ochterski JW, Martin RL, Morokuma K, Farkas O, Foresman JB, Fox DJ: *Gaussian 16 rev. A.03, wallingford, CT*. 2016.

50. Mulliken RS: **Electronic population analysis on LCAO–MO molecular wave functions. I**. *J Chem Phys* 1955, **23**:1833–1840.

51. Kornyshev AA, Vorotyntsev MA, Nielsen H, Ulstrup J: **Non-local screening effects in the long-range interionic interaction in a polar solvent**. *J Chem Soc Faraday Trans* 1982, **2 78**:217–241.

52. Iversen G, Kharkats YuI, Ulstrup J: **Simple dielectric image charge models for electrostatic intesactions in metalloproteins**. *Mol Phys* 1998, **94**:297–306.